Systems/Circuits

Regional Delta Waves In Human Rapid Eye Movement Sleep

Giulio Bernardi,[1,2] Monica Betta,[2] Emiliano Ricciardi,[2] Pietro Pietrini,[2] Giulio Tononi,[3] and Francesca Siclari[1]

[1]Center for Investigation and Research on Sleep, Lausanne University Hospital, CH-1011 Lausanne, Switzerland, [2]MoMiLab Research Unit, IMT School for Advanced Studies, IT-55100 Lucca, Italy, and [3]Department of Psychiatry, University of Wisconsin, Madison, Wisconsin 53719

Although the EEG slow wave of sleep is typically considered to be a hallmark of nonrapid eye movement (NREM) sleep, recent work in mice has shown that slow waves can also occur in REM sleep. Here, we investigated the presence and cortical distribution of negative delta (1–4 Hz) waves in human REM sleep by analyzing high-density EEG sleep recordings obtained in 28 healthy subjects. We identified two clusters of delta waves with distinctive properties: (1) a frontal-central cluster characterized by ~2.5–3.0 Hz, relatively large, notched delta waves (so-called "sawtooth waves") that tended to occur in bursts, were associated with increased gamma activity and rapid eye movements (EMs), and upon source modeling displayed an occipital-temporal and a frontal-central component and (2) a medial-occipital cluster characterized by more isolated, slower (<2 Hz), and smaller waves that were not associated with rapid EMs, displayed a negative correlation with gamma activity, and were also found in NREM sleep. Therefore, delta waves are an integral part of REM sleep in humans and the two identified subtypes (sawtooth and medial-occipital slow waves) may reflect distinct generation mechanisms and functional roles. Sawtooth waves, which are exclusive to REM sleep, share many characteristics with ponto-geniculo-occipital waves described in animals and may represent the human equivalent or a closely related event, whereas medial-occipital slow waves appear similar to NREM sleep slow waves.

Key words: hd-EEG; PGO wave; REM sleep; sawtooth wave; slow wave

Significance Statement

The EEG slow wave is typically considered a hallmark of nonrapid eye movement (NREM) sleep, but recent work in mice has shown that it can also occur in REM sleep. By analyzing high-density EEG recordings collected in healthy adult individuals, we show that REM sleep is characterized by prominent delta waves also in humans. In particular, we identified two distinctive clusters of delta waves with different properties: a frontal-central cluster characterized by faster, activating "sawtooth waves" that share many characteristics with ponto-geniculo-occipital waves described in animals and a medial-occipital cluster containing slow waves that are more similar to NREM sleep slow waves. These findings indicate that REM sleep is a spatially and temporally heterogeneous state and may contribute to explaining its known functional and phenomenological properties.

Introduction

Sleep is characterized by relative quiescence and reduced responsiveness to external stimuli. Based on electrophysiological hallmarks, sleep is divided into non-rapid eye movement (NREM) sleep and REM sleep. Although REM sleep is characterized by rapid eye movements (EMs) and muscular atonia and by a tonically "activated" (low-voltage, high-frequency) EEG resembling that of wakefulness (Aserinsky and Kleitman, 1953; Dement and Kleitman, 1957), hallmarks of NREM sleep include high-amplitude, slow waves (≤4 Hz) and spindles (12–16 Hz) (Steriade et al., 1993, 2001). Given these differences, it has been commonly assumed that wakefulness, NREM sleep, and REM sleep represent mutually exclusive "global" states. This view has been recently challenged by a growing body of evidence indicating that many features of sleep are essentially local and that islands of sleep- and wake-like activity may coexist in different brain areas (Siclari and Tononi, 2017).

EEG slow waves of NREM sleep occur when neurons become bistable and oscillate between two states: a hyperpolarized down-state characterized by neuronal silence (off-period), and a depolarized up-state during which neurons fire (on-period) (Steriade et al., 2001). Intracranial recordings in humans have shown that,

Received Sept. 5, 2018; revised Nov. 28, 2018; accepted Jan. 4, 2019.

Author contributions: G.B., E.R., P.P., G.T., and F.S. designed research; G.B. and F.S. performed research; G.B., M.B., and F.S. analyzed data; G.B., M.B., and F.S. wrote the first draft of the paper; G.B., M.B., E.R., P.P., G.T., and F.S. edited the paper; G.B. and F.S. wrote the paper.

This work was supported by the Swiss National Science Foundation (Ambizione Grant PZ00P3_173955 to F.S.), the Divesa Foundation Switzerland (F.S.), the Pierre-Mercier Foundation for Science (F.S.), the Bourse Pro-Femme of the University of Lausanne (F.S.), and the Foundation for the University of Lausanne (F.S., G.B.). We thank Brady Riedner, Michele Bellesi, Joshua J. LaRocque, and Xiaoqian Yu for technical assistance and help with data collection.

The authors declare no competing financial interests.

Correspondence should be addressed to Francesca Siclari at francesca.siclari@chuv.ch or Giulio Bernardi at giuliobernа@gmail.com.

https://doi.org/10.1523/JNEUROSCI.2298-18.2019

during stable NREM sleep, slow waves can be restricted to some localized areas and occur out of phase with other cortical regions (Nir et al., 2011). The regional distribution of slow-wave activity (SWA) has been shown to be modulated by recent experience and learning (Huber et al., 2004, 2006). Local slow waves, involving small portions of the cortical mantle, have also been shown to occur in awake humans (Hung et al., 2013; Bernardi et al., 2015) and rodents (Vyazovskiy et al., 2011, 2014), particularly in conditions of sleep deprivation. Importantly for the purposes of our study, recent work demonstrated that, in mice (Funk et al., 2016), slow waves with neuronal off-periods may also occur during REM sleep in primary visual (V1), sensory (S1), and motor (M1) areas, mainly in cortical layer 4. By contrast, associative areas such as V2, S2, or the retrosplenial cortex showed the typical activated pattern of REM sleep. It is currently unknown whether similar regional differences and local slow waves also exist in human REM sleep. In fact, whereas great effort has been dedicated to the study of prominent features of REM sleep such as theta (5–8 Hz) or high-frequency (>25 Hz) activity, little attention has been given to delta (≤4 Hz) waves during this sleep stage. A few studies found that delta power (1–4 Hz) in REM sleep had a different topographic distribution with respect to NREM sleep (Tinguely et al., 2006; Ferrara and De Gennaro, 2011). In addition, we recently showed that, in both REM and NREM sleep, reduced delta power in posterior cortical regions is associated with dreaming (Siclari et al., 2017), suggesting a similar functional significance of slow waves across states. By analyzing slow-wave characteristics in NREM sleep, we identified two types of slow waves with distinct features: large, steep frontal-central type I slow waves, which are likely generated in a bottom-up manner by arousal systems, and smaller type II slow waves, which are diffusely distributed over the cortical mantel and probably underlie a corticocortical synchronization mechanism (Siclari et al., 2014). Further analyses showed that the two types of slow waves are differentially related to dreaming (Siclari et al., 2018).

In the present study, we investigated the presence and cortical distribution of delta (1–4 Hz) waves in human REM sleep using high-density EEG (hd-EEG) recordings, which provide an excellent combination of temporal and spatial resolution. We also wanted to determine whether we could identify different delta wave types with distinct characteristics similar to those in NREM sleep. The "sawtooth waves" of REM sleep, for instance, are known to peak in the delta range (~3 Hz), but their properties and cortical distributions have not been systematically investigated in humans using techniques with a high spatial resolution. Therefore, we expected to identify at least two types of delta waves in human REM sleep, corresponding to sawtooth waves and local slow waves involving primary sensory cortices.

Materials and Methods

Participants. Overnight hd-EEG recordings (Electrical Geodesics, 256 electrodes, 500 Hz sampling frequency) were obtained in 16 healthy volunteers (age 24.9 ± 4.5, 8 females; 13 right-handed). NREM sleep data (but not REM sleep data) from 10 of these subjects have been reported previously (Bernardi et al., 2018). All participants had a sleep duration of ~7 h/night, consistent bed/rise times, no daytime nap habits, and no excessive daytime sleepiness (total scores in the Epworth Sleepiness Scale ≤10; Johns, 1991). A clinical interview was performed to exclude a history of sleep, medical, and psychiatric disorders. The study was approved by the institutional review board (IRB) of the University of Wisconsin–Madison. Each participant signed an IRB-approved informed consent form before enrollment.

Because wake data were not available for the above subjects, specific analyses aimed at comparing sleep- and wake-related brain activity (see below) were performed in a different sample of 12 healthy adult individuals (age 25.5 ± 3.7, 6 females) who underwent overnight hd-EEG sleep recordings after having spent 8 h in the sleep laboratory while watching movies (analyses of wake and NREM sleep data from these subjects has been reported previously (Bernardi et al., 2019). These recordings were performed at the Lausanne University Hospital under a research protocol approved by the local ethical committee.

Table 1. Sleep parameters for the 16 subjects included in the study

Parameter ($N = 16$)	Average	SD
Total sleep time (min)	397.5	79.8
N1 time (min)	21.8	15.2
N1 proportion (%)	5.6	4.2
N2 time (min)	209.5	52.1
N2 proportion (%)	52.9	9.0
N3 time (min)	78.0	29.6
N3 proportion (%)	20.0	6.5
REM time (min)	88.3	33.3
REM proportion (%)	21.5	6.1
REM latency (min)	91.5	33.5
REM cycles (no.)	4.0	1.4

EEG data preprocessing. All hd-EEG recordings (Madison dataset) were first-order high-pass filtered at 0.1 Hz and band-pass filtered between 0.5 and 58 Hz. For scoring purposes, four of the 256 electrodes, two placed at the outer canthi of the eyes, and two placed above and below one of the two eyes, were used to monitor EMs (EOG), whereas electrodes located in the chin–cheek region were used to evaluate muscular activity (EMG). Sleep scoring (Table 1) was performed over 30 s epochs according to standard criteria by a physician board-certified in sleep medicine (Iber et al., 2007). All the epochs scored as REM sleep were identified and extracted.

Detection and classification of delta waves. For each subject and recording, channels containing artifactual activity were visually identified, rejected, and replaced with data interpolated from nearby channels using spherical splines (NetStation' Electrical Geodesics). Potential ocular, muscular, and electrocardiograph artifacts were removed using independent component analysis (ICA) in EEGLAB (Delorme and Makeig, 2004). An algorithm based on the analysis of consecutive signal zero-crossings (Riedner et al., 2007) was adapted for the detection of delta waves in REM sleep. Before application of the algorithm, the signal of each channel was referenced to the average of the two mastoid electrodes, down-sampled to 128 Hz, and filtered between 1 and 10 Hz (the upper limit of the filter was selected to minimize wave shape and amplitude distortions). For each detected half-wave with a duration between 125 and 500 ms (1–4 Hz), the following properties were extracted and stored for further analyses: negative amplitude (μV), duration (ms) and number of negative peaks (np/w). As described in previous work (Riedner et al., 2007), the negative peaks were identified based on the zero crossings of the EEG signal derivative corresponding to the negative half-wave after application of a 50 ms moving-average filter. The density of slow waves (waves per minute; w/min) was also computed.

Preliminary analyses revealed two spatially distinct clusters of low-frequency waves in the 1–4 Hz range: a frontal-central and a medial-occipital cluster characterized by different frequencies and amplitudes (see Fig. 1). For this reason, subsequent analyses were in part adapted to the characteristics of the two delta wave types (see Results).

Temporal clusterization of delta waves. We investigated the tendency of delta waves to occur in bursts. Bursts were defined as a series of at least three consecutive waves with maximum negative peaks <750 ms apart. For this analysis, a slightly broader half-wave duration limit (range 1–5 Hz) was used to minimize exclusion of potential "borderline" delta waves within a burst. An amplitude constraint was applied so that the amplitude of each consecutive wave in the burst had to vary by <25% (relative to the preceding wave). No other amplitude or duration threshold was applied.

Relationship with rapid EMs. Individual rapid EMs were identified using an automatic detection algorithm (Betta et al., 2013, 2015). In brief,

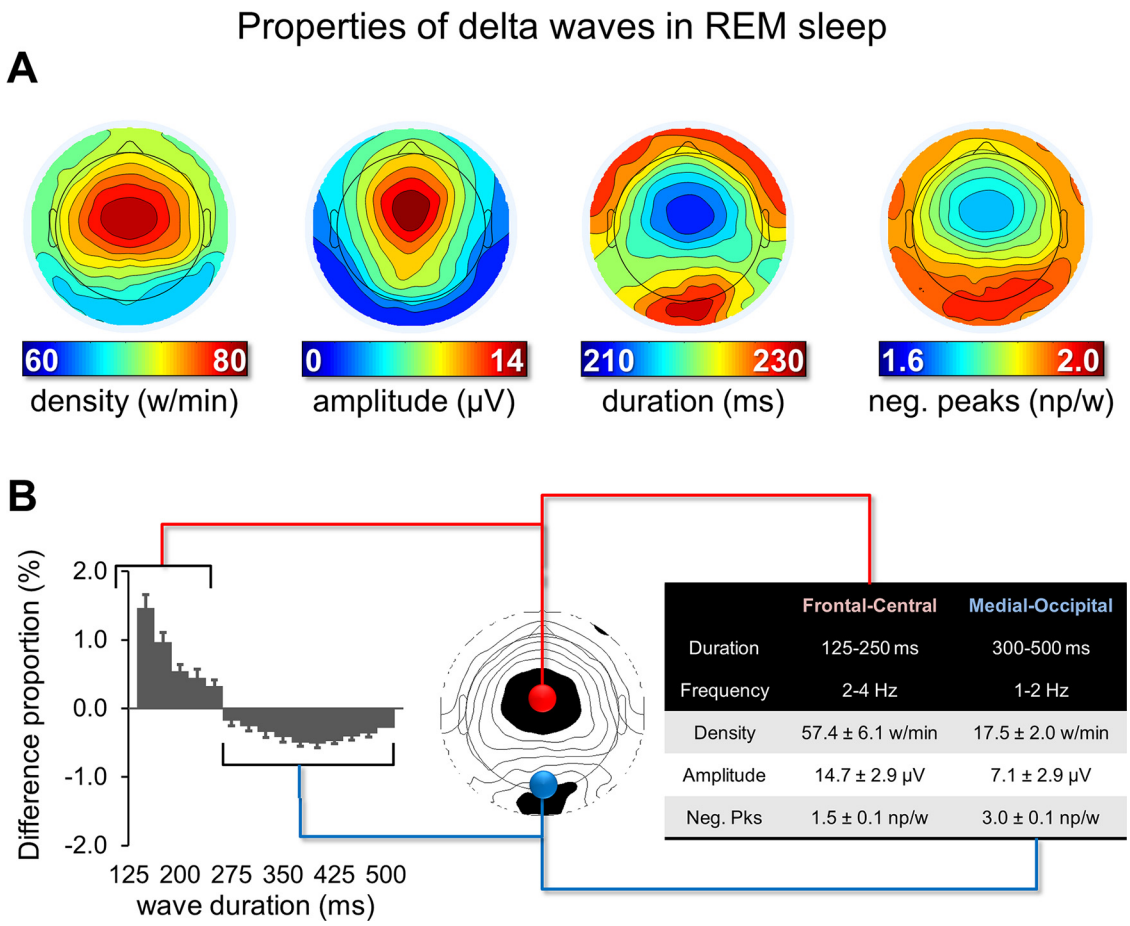

Figure 1. Properties of delta waves in REM sleep. An automatic detection algorithm was applied to the EEG signal of each electrode to identify negative half-waves with a duration of 125–500 ms (≤4 Hz). Different wave properties were extracted and analyzed (***A***), including density (number of waves per minute; w/min), negative amplitude (μV), duration (ms), and number of negative peaks (np/w). A similar distribution was obtained for negative peaks when values were expressed per second instead of per wave, although the highest values were found in more lateral posterior rather than medial posterior regions. ***B***, Left, For a frontal-central and a medial-occipital electrode, the difference (%) in the relative proportion of waves for durations between 125 and 500 ms (25 ms bins). The relative difference between the two electrodes in percentage was calculated for each duration bin. Vertical bars indicate 1 SD from the group mean (SD). The table on the right side displays mean values and SD for density, amplitude and negative peaks (neg. pks) for the faster frontal-central and the slower medial-occipital delta waves.

the algorithm detects local peaks in the sum of the Haar wavelet transform coefficients in a specific frequency range (0.8–5 Hz) to determine the exact timing and duration of each EM (Betta et al., 2013). Bursts of rapid EMs were defined as serial EMs (2 or more) separated by <1 s. Isolated rapid EMs/bursts were defined as single EMs/bursts preceded and followed by periods of at least 5 s without rapid EMs. To determine how delta waves relate to rapid EMs, for each isolated EM, wave density was calculated in two windows corresponding to 1 s before the onset of the first EM ("pre") and 1 s after the end of the last EM ("post").

Phasic REM periods were defined as time periods longer than 5 s that were occupied by EMs for >50% of their length. EMs in this time window had to be <2 s apart to be considered as part of the same phasic period. Tonic REM episodes were defined as time periods longer than 5 s that were completely free from any EMs. The average density of frontal-central and medial-occipital waves was calculated in all phasic and tonic periods.

To increase the signal-to-noise ratio of these analyses, amplitude thresholds corresponding to 10 and 3 μV were applied for frontal-central and medial-occipital delta waves, respectively.

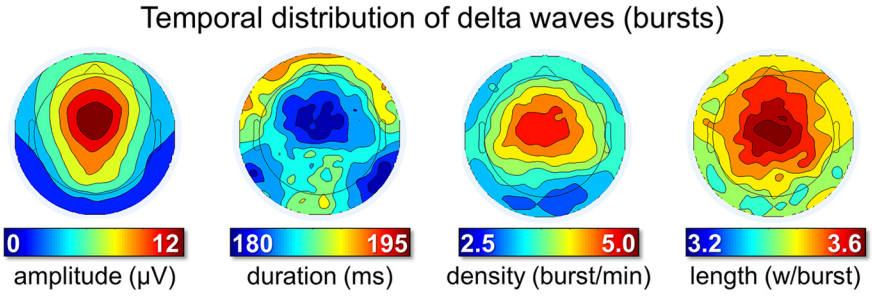

Figure 2. Temporal distribution of delta waves (occurrence in bursts). Bursts were defined as series of at least 3 consecutive waves (1–5 Hz) with maximum negative peaks separated by <750 ms. From left to right, the plots display the density of delta wave bursts (number of bursts per minute), the mean amplitude (μV), and duration (ms) of waves included in a burst and the number of waves included in the burst (expressed as waves per burst).

Relationship with high-frequency activity. Next, in light of previous observations linking NREM slow waves to changes in high-frequency EEG activity (Valderrama et al., 2012; Siclari et al., 2014), we examined the temporal relation between gamma and delta power during delta waves of REM sleep. For each wave, the band-specific instantaneous signal power was computed as the root mean square (RMS, time window = 40 ms, step = 20 ms) of the delta (0.5–4 Hz) and gamma band-pass filtered (30–55 Hz) signals in a 2 s time window centered on the negative peak of the delta wave. To increase the signal-to-noise ratio,

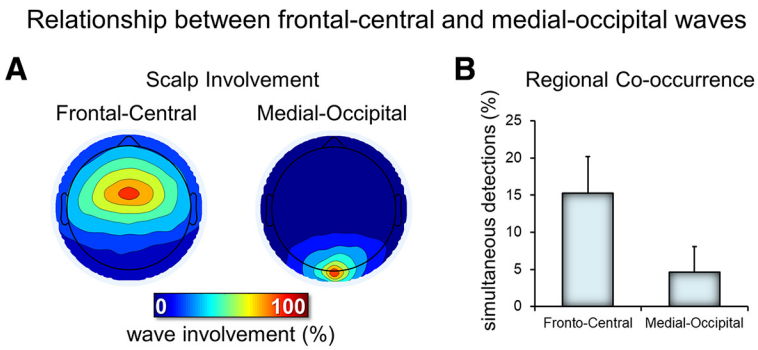

Figure 3. Relationship between frontal-central and medial occipital delta waves. ***A***, Typical scalp involvement for the two types of delta waves. For each delta wave detected in the two electrodes of interest (frontal-central and medial-occipital), the number of concurrent detections (in a window of 200 ms, centered on the wave negative peak) in other electrodes was computed. Therefore, each map shows the number of cases in which each electrode showed a co-occurring delta wave (the electrode of interest has 100% value in each map). ***B***, Relative occurrence of simultaneous detections (of the same type/duration) across the two electrodes of interest.

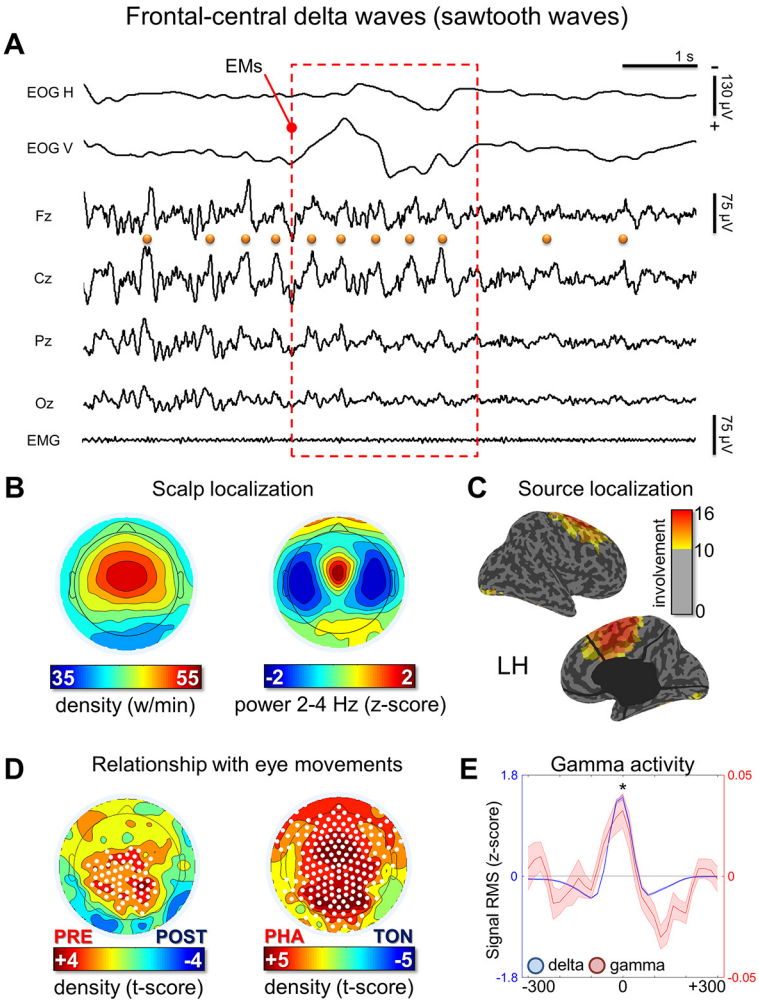

Figure 4. Frontal-central delta waves. ***A***, Representative REM sleep EEG traces (negative-up on the *y*-scale) containing frontal-central delta waves with a duration of 125–250 ms (half-wave). The orange dots indicate waves identified by the automatic detection algorithm in the Cz electrode and the red box marks the occurrence of EMs. Most waves corresponded to typical notched sawtooth waves of REM sleep. ***B***, Density- and power-based maps indicating their topographic distribution. Power spectral density (PSD) was calculated in 6 s epochs and across all REM cycles using the Welch's method (8 sections, 50% overlap) and integrated in the frequency range of interest. ***C***, Typical peak of activity of frontal-central waves in source space (overlap between subjects). ***D***, Comparison between wave density before and after isolated EMs and between phasic and tonic REM periods. ***E***, Relationship between delta and gamma activity (RMS of band-limited signal). RMS traces were aligned using the maximum negative peak of each wave as a reference. Asterisk marks a significant increase of gamma activity at the wave peak with respect to baseline ($p < 0.05$).

amplitude thresholds corresponding to 10 and 3 μV were applied for frontal-central and medial-occipital delta waves, respectively. For each subject, delta and gamma RMS time series were *z*-score transformed in a 600 ms time window centered on the wave negative peak and then averaged across all of the detected waves.

Overnight changes in delta waves. Slow waves of NREM sleep are known to change in density and amplitude across a night of sleep (Riedner et al., 2007; Bernardi et al., 2018). Therefore, here, we evaluated whether delta waves of REM sleep undergo similar changes. Specifically, for each subject, we first calculated the mean density and amplitude of delta waves within each REM sleep cycle. Then, the magnitude of the density/amplitude changes ("slope") was calculated across cycles using least square linear regression (considering as independent variable the absolute sleep time at half of the corresponding REM sleep cycle).

Relationship with delta waves of NREM sleep. To evaluate similarities and differences between delta waves of REM and NREM sleep, additional analyses were performed on a subsample of 10 subjects (4 females, age 25.4 ± 4.7). NREM data of these 10 subjects were preprocessed using the same procedures described above as part of a previous study aimed at exploring different types of slow waves during NREM sleep (Bernardi et al., 2018). For these subjects, the same negative half-wave detection algorithm described above was applied to N2 and N3 sleep data of the whole night on a channel-by-channel basis. Then, half-waves with duration 125–250 ms (>2 Hz) and 300–500 ms (<2 Hz) were identified to calculate mean density (w/min) and negative amplitude (μV). A nonparametric Friedman test was applied to investigate potential stage-dependent (N2/N3/REM) differences in these parameters.

Specificity of REM sleep delta waves with respect to wakefulness. To verify whether delta waves of REM sleep are specific to this stage or if they are also observed in wakefulness, additional analyses were performed using REM and waking (rest with eyes closed) data collected in 12 healthy adults (6 females, age 25.5 3.7; Bernardi et al., 2019). These recordings were preprocessed as described previously, but a 0.5–45 Hz band-pass filter was used in this case. Moreover, resting-state recordings in wakefulness were initially divided into nonoverlapping 5 s epochs and visually inspected to identify and reject epochs containing clear artifacts before application of the ICA procedure. A nonparametric Wilcoxon signed-rank test was used to compare amplitude and density of delta waves across REM sleep and wakefulness.

Source modeling analysis. A source modeling analysis was performed to determine the cortical involvement of delta waves in REM sleep. First, the negative-going envelope of the EEG signal was obtained by selecting the second-most negative sample across 65 channels included in a medial frontal-central or in a temporo-occipital region of interest (Siclari et al., 2014; Mensen et al., 2016). The resulting signal was broadband filtered (0.5–40 Hz,

stop-band at 0.1 and 60 Hz) and the same negative half-wave detection algorithm described above was applied. Specific criteria were applied to further select waves with typical properties of frontal-central and medial-occipital waves and to optimize source estimation while minimizing the potential impact of residual noise. In particular, anterior waves with a negative amplitude >20 μV and a duration of 125–375 ms and posterior waves with a negative amplitude of 5–50 μV and a duration >300 ms were analyzed. The duration ranges applied here were broader than those reported for the other analyses at the single-channel level to take into account potential wave propagation (Massimini et al., 2004; Mensen et al., 2016). For the analysis of frontal-central waves, the EEG signal was filtered between 2 and 5 Hz (stop band at 1.5 and 6 Hz), whereas it was filtered between 0.5 and 2.5 Hz (stop band at 0.1 and 4 Hz) for medial-occipital waves. Then, source localization was performed on 1 s data segments centered on the negative peak of each delta wave using GeoSource (NetStation; Electrical Geodesics). A four-shell head model based on the Montreal Neurological Institute atlas and a standard coregistered set of electrode positions were used to construct the forward model. The inverse matrix was computed using the standardized low-resolution brain electromagnetic tomography (sLORETA) constraint. A Tikhonov regularization procedure (10^{-2}) was applied to account for the variability in the signal-to-noise ratio. The source space was restricted to 2447 dipoles distributed over 7 mm^3 cortical voxels. For each delta wave, the cortical involvement was computed as the average of the relative current density achieved within a time window of 20 ms around the wave negative peak. Finally, for each subject, the probabilistic involvement was defined as the probability for each voxel to be among the 25% of voxels showing the maximal cortical involvement.

Experimental design and statistical analysis. All statistical analyses were performed using MATLAB (The MathWorks) or SPSS Statistics (IBM).

Statistical comparisons between phasic and tonic REM periods or between pre- and post-EM periods were performed using parametric paired *t* tests including all study participants ($N = 16$; Madison dataset). The relationship between the number of delta waves and the number of rapid EMs was investigated using the Spearman's correlation coefficient. A nonparametric, permutation-based test was used to evaluate significance of overnight amplitude and density changes in delta waves. Nonparametric Friedman's tests were applied to identify potential differences across sleep stages (N2, N3, REM) and Wilcoxon signed-rank tests were used for paired comparisons with relatively small sample sizes ($n = 10$ or $n = 12$).

When hypotheses were tested across multiple voxels/electrodes, a nonparametric approach based on the definition of a cluster-size-threshold was used to control for multiple comparisons (Nichols and Holmes, 2002; Fattinger et al., 2017). Specifically, a null distribution was generated by randomly relabeling the condition label from the original data for group-level comparisons and by randomly reordering observations for correlation analyses ($n = 1000$ permutations). For each permutation, the maximal size of the resulting clusters reaching an (uncorrected) significance threshold of $p < 0.05$ was included in the cluster-size distribution. Then, the 95th percentile (5% significance level) was determined as the critical cluster-size threshold.

Results

Topographic analysis of delta waves in REM sleep

First, we evaluated the topographic distribution of the density, amplitude, duration, and negative peaks of all negative waves detected in the 1–4 Hz range (Fig. 1*A*). We identified two spatially distinct clusters with different properties: a frontal-central cluster in which waves had a relatively high density, a high amplitude, a low duration, and a low number of negative peaks and a medial-occipital cluster characterized by fewer waves with a lower amplitude, a longer duration, and a higher number of negative peaks. Next, we selected a representative electrode for each of the two clusters (channel 8, corresponding to the channel between Fz and Cz, and channel 137, corresponding to Oz) and compared the distribution of wave density as a function of their duration between the two channels (Fig. 1*B*, left). This analysis

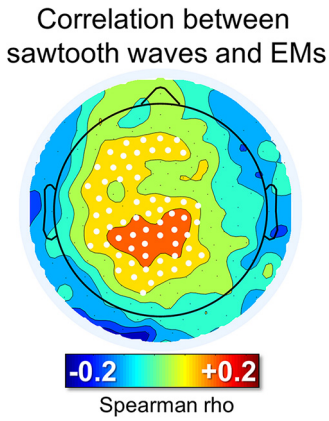

Figure 5. Correlation between the number of sawtooth waves preceding rapid EMs and the number of subsequent rapid EMs. For each isolated group of EMs, the burst of the 125–250 ms half-waves (amplitude > 10 μV, interwave distance < 1 s) closest to the beginning of the first EM (maximum distance < 600 ms) was identified. White dots mark significant effects at the group level ($p < 0.05$, corrected).

confirmed that the frontal cluster contained more faster waves (125–250 ms, >2 Hz), whereas the medial-occipital cluster contained more slower waves (300–500 ms, <2 Hz). Mean values for density, amplitude, and negative peaks for characteristic faster frontal-central waves (125–250 ms) and slower medial-occipital waves (300–500 ms) are shown in Figure 1*B* (right). Next, to better characterize the temporal dynamics of the occurrence of delta waves, we evaluated the topographic distribution of wave parameters only for delta waves occurring in bursts (see Materials and Methods for details). This analysis revealed that waves occurring in bursts were mainly found in the frontal-central cluster and had similar characteristics to the frontal-central waves described above (Fig. 2). For subsequent analyses, we distinguished between frontal-central faster waves lasting 125–250 ms and medial-occipital slower waves lasting 300–500 ms. We found that both types of waves were essentially local, as indicated by the mean proportion of recruited channels (32.0 ± 4.0% for frontal-central waves and 9.5 ± 3.5% for medial-occipital waves; Fig. 3) and by the low probability of simultaneous detections in the frontal-central and in the medial-occipital electrode (15.2 ± 5.0% and 4.6 ± 3.5%, respectively). Importantly, faster frontal-central and slower medial-occipital waves tended to occur independently from each other: for each wave type, co-occurrence with the other wave type across the frontal-central and the medial-occipital electrode was observed for only 4.9 ± 1.3% and 16.4 ± 4.3% of all delta waves, respectively. Given that the observed values are closer to 0% than to 100%, our results suggest the existence of distinct generators for the two wave types.

Faster frontal-central waves (sawtooth waves)

Visual inspection of these waves revealed that many of them looked like the typical sawtooth waves of REM sleep (Fig. 4*A*), displaying a notch either before or after the maximum negative peak. These waves showed a frequency peak between 2.5 and 3 Hz and a maximum power between the vertex (Cz) and frontal (Fz) electrodes (Fig. 4*A*,*B*). It should be noted that, in some studies, sawtooth waves have been described as having a positive polarity (i.e., recognizing the positive component as prominent; (Yasoshima et al., 1984; Sato et al., 1997), whereas others have regarded sawtooth waves as negative waves (Rodenbeck et al., 2006). In fact, sawtooth waves often present a relatively symmetrical distribution around the zero voltage baseline. In the present

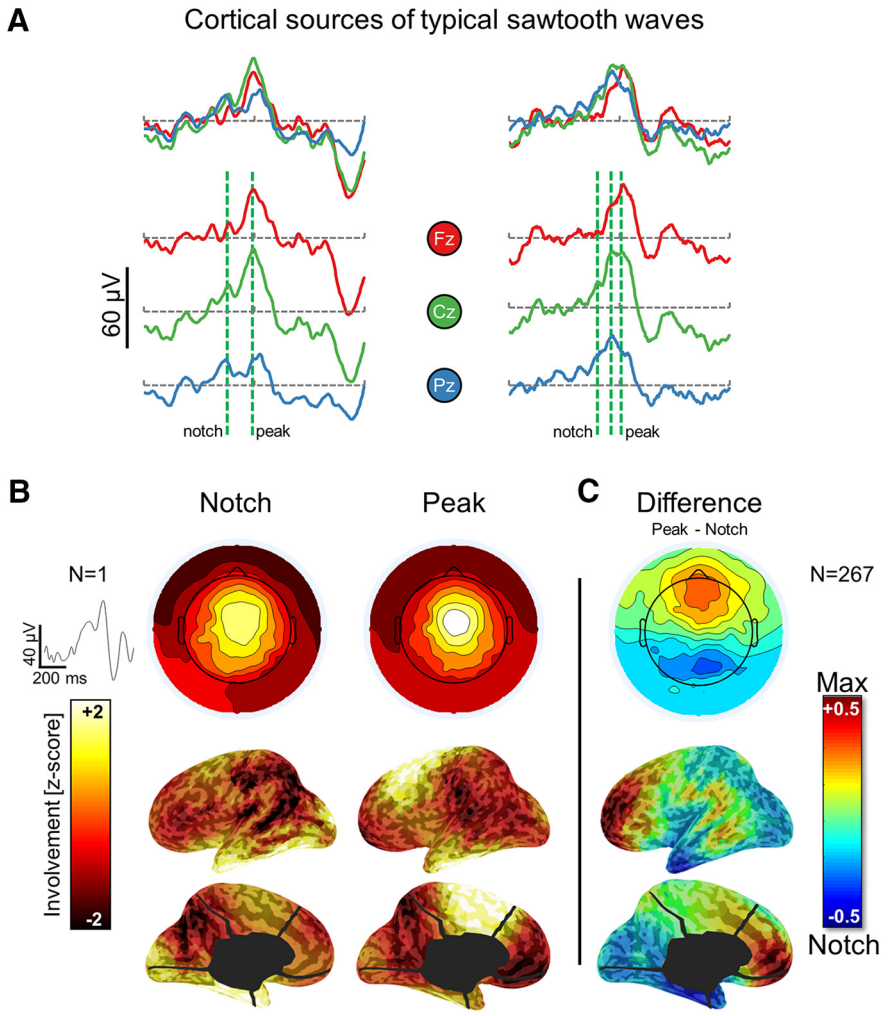

Figure 6. Cortical sources of typical sawtooth waves. ***A***, EEG traces (three electrodes, corresponding to Fz, Cz, and Pz; negative-up on the *y*-scale) of two representative notched sawtooth waves (±250 ms around the negative peak of the algorithm detection). ***B***, Scalp and cortical involvement corresponding to the notch and the maximal negative peak of a single sawtooth wave. ***C***, Difference in average involvement between the notch and maximal negative peak (computed across 267 sawtooth waves in one representative subject; similar results were obtained in other participants). For this evaluation, all detections in one subject were visually inspected to identify typical sawtooth waves with a negative amplitude >20 μV and a well recognizable notched, triangular shape. The timing of the notch and the maximal negative peak were marked manually. Differences shown in ***C*** are statistically significant over all voxels ($p < 0.05$, corrected).

work, only negative half-waves were specifically included (Rodenbeck et al., 2006). Source modeling of the signal corresponding to the maximum negative peak revealed the greatest overlap between subjects (>10) in a medial frontal area comprising the midcingulate gyrus, the supplementary motor area (SMA), and the medial part of the primary motor (M1) cortex (Fig. 4*C*). Sawtooth waves displayed a clear density increase before rapid EM and during phasic REM periods (Fig. 4*D*), which is consistent with previous observations in both human subjects and primates (Berger et al., 1962; Schwartz, 1962; Snyder et al., 1978; Sato et al., 1997; Pearl et al., 2002; Takaharaa et al., 2009). A direct positive correlation between the number of sawtooth waves preceding the EMs and the number of associated EMs was also observed (Fig. 5). Finally, the analysis of gamma activity during sawtooth waves revealed a positive, in-phase association between low- and high-frequency EEG activity (Fig. 4*E*).

Next, given the notched appearance of typical sawtooth waves (Rodenbeck et al., 2006), we evaluated the topographic and cortical distribution of the signal during the notch and maximum negative peak of the wave separately. Specifically, for each detected wave presenting characteristics of sawtooth waves, we visually identified the timing of the most prominent secondary peak occurring on the negative slope (from positive to negative) of the wave. This analysis, applied at the scalp and source level, revealed that the notched appearance results from the superimposition of two cortical sources: a frontal-central source corresponding to the maximal negative peak of the sawtooth wave involving the midcingulate, medial, and superior frontal areas (including motor and premotor regions) and a posterior source corresponding to the notch of the wave involving occipital and inferior temporo-occipital areas. Results from one representative subject are shown in Figure 6. For consistency, only sawtooth waves with a notch preceding the maximum negative peak were visually identified for this analysis, although sometimes a notch could also be observed following the maximum negative peak.

Slow medial-occipital waves

Visual inspection of EEG traces revealed that the great majority of slow (300–500 ms) medial-occipital waves corresponded to shallow negative deflections, frequently accompanied by faster, superimposed theta-alpha activity (Fig. 7*A*). These waves showed their maximum power in the occipital cortex (Fig. 7*A*,*C*) and did not display clear changes in relation to rapid EM. However, they showed a relative decrease in frontal-central, but not in occipital, areas during phasic versus tonic REM sleep periods (Fig. 7*D*). Similar to slow waves in NREM sleep (Siclari et al., 2014), REM slow waves were associated with a decrease in gamma activity (Fig. 7*E*).

Overnight changes in delta waves

An analysis of overnight changes in wave amplitude revealed a significant, non-region-specific (i.e., both frontal and occipital) and non-frequency-specific (i.e., for both faster and slower waves) decrease across the night (Fig. 8). No overnight changes in wave density were observed.

Relationship with delta waves of NREM sleep

We then investigated whether waves with sawtooth and medial-occipital characteristics were specific to REM sleep or if they could also occur in NREM sleep. We found that the density of delta waves in the sawtooth frequency range differed significantly between stages (Friedman test $p < 0.0001$, $\chi^2 = 20.0$) in the frontal-central region, being maximal in REM sleep and lowest in N3 sleep ($p < 0.005$, $|z| = 2.803$; Wilcoxon signed-rank test). Instead, the density of slower waves in the medial-occipital cluster did not change significantly across sleep stages (Friedman test $p > 0.05$, $\chi^2 = 5.4$; Fig. 9). Amplitude was significantly higher in N2 and N3 sleep than in REM sleep for both faster frontal-central

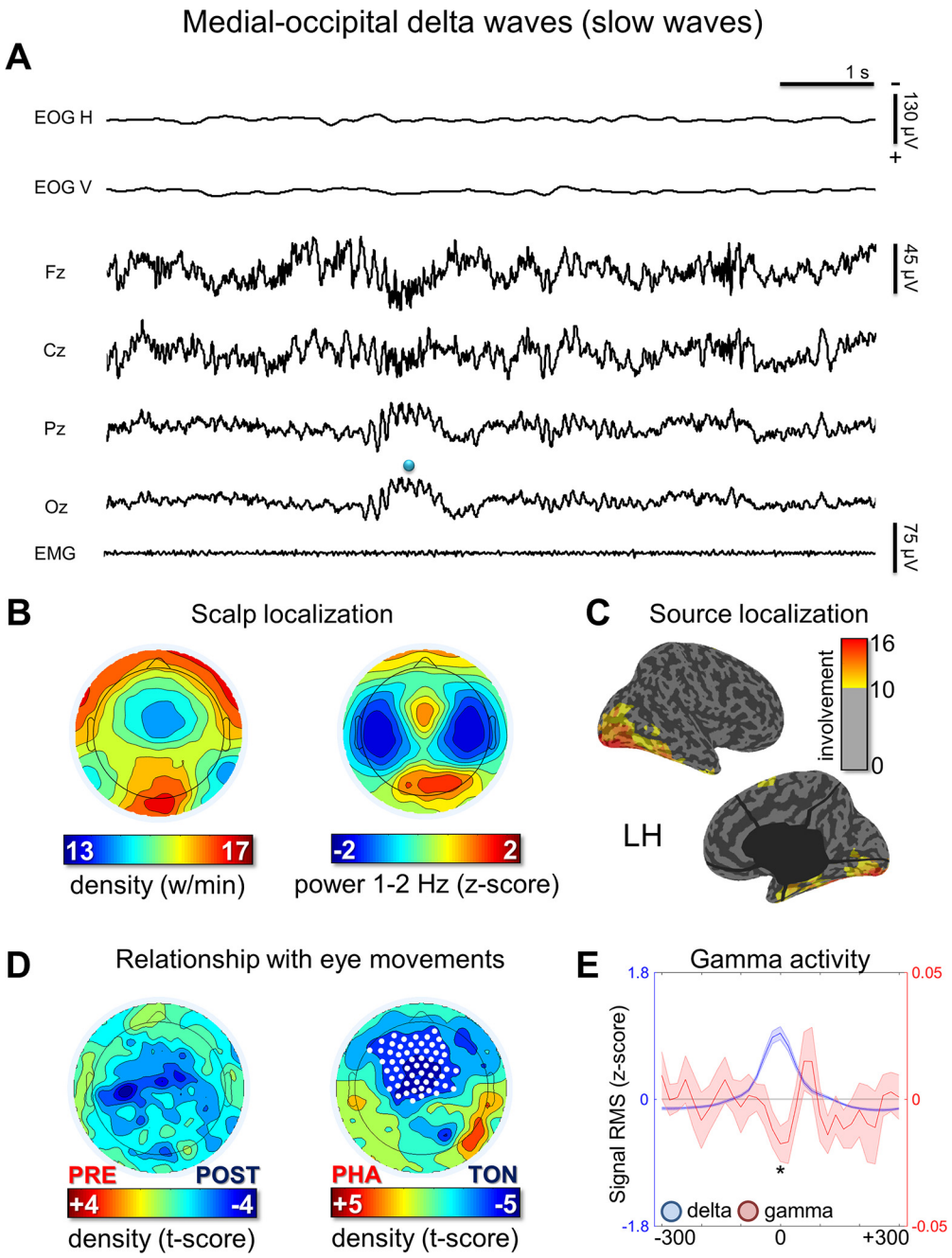

Figure 7. Medial-occipital delta waves. ***A***, Representative REM sleep EEG traces (negative-up on the *y*-scale) containing medial-occipital delta waves with a duration of 300–500 ms (half-wave). The blue dot indicates a wave identified by the automatic detection algorithm in the Oz electrode. ***B***, Density- and power-based maps indicating their topographic distribution. Power spectral density (PSD) was calculated in 6 s epochs and across all REM cycles using the Welch's method (8 sections, 50% overlap) and integrated in the frequency-range of interest. ***C***, Typical peak of activity of medial-occipital waves in source space (overlap between subjects). ***D***, Comparison between medial-occipital wave density before and after isolated EMs and between phasic and tonic REM-periods. ***E***, Relationship between delta and gamma activity (RMS of band-limited signal). RMS traces were aligned using the maximum negative peak of each wave as a reference. Asterisk marks a significant decrease of gamma activity at the wave peak with respect to baseline ($p < 0.05$).

waves (Friedman test $p < 0.0001$, $\chi^2 = 16.8.0$) and slower medial-occipital waves (Friedman test $p < 0.0001$, $\chi^2 = 20.0$). For a topographic display of waves across stages, see Figure 10.

Relationship with delta waves of wakefulness

Because we found that the slower medial occipital waves were not specific to REM sleep, but also occurred with a similar incidence in NREM sleep, we investigated whether they were also present in wakefulness. We performed an additional analysis in a different dataset containing both REM sleep and wake data (2 min of relaxed wakefulness obtained with eyes closed in the morning). This analysis showed that medial-occipital slow waves had a significantly lower density ($p < 0.005$, $|z| = 3.059$) in wakefulness relative to REM sleep. Specifically, the average density was 5.5 ± 2.8 w/min in awake subjects and 14.1 ± 1.6 w/min during REM sleep (across the whole night), suggesting that they are clearly modulated by the change in behavioral state (sleep vs wakefulness). Wave amplitude was similar across conditions ($p = 0.272$, $|z| = 1.098$). The same analysis performed for faster frontal-central waves showed that these waves had a higher density ($p <$

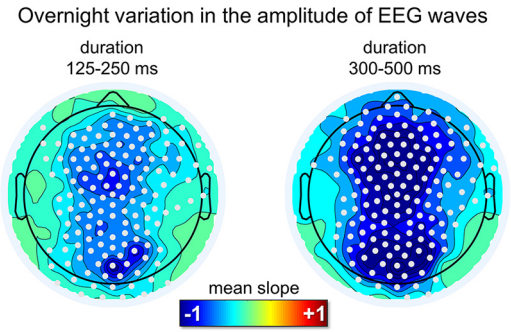

Figure 8. Overnight changes in the amplitude of delta waves in REM sleep for the sawtooth frequency range (125–250 ms) and the medial-occipital wave range (300–500 ms). A diffuse decrease in amplitude was observed for both frequency ranges. White dots mark significant effects at the group level ($p < 0.05$, corrected).

0.005, $|z| = 3.059$) and amplitude ($p < 0.005$, $|z| = 2.903$) in REM sleep relative to wakefulness. The average density of frontal-central waves was 34.0 ± 4.7 w/min in awake subjects and 54.1 ± 7.1 w/min during REM sleep.

Discussion

Here, we show that delta waves (≤4 Hz) are an integral part of human REM sleep. By analyzing delta wave properties separately, two distinct spatial clusters emerged spontaneously: a frontal-central cluster with frequent, faster (2–4 Hz), 'high'-amplitude waves and a medial-occipital cluster with isolated, slower (<2 Hz), low-amplitude waves. Both waves were essentially local, involving only a minority of channels, and occurred independently from one another.

Frontal-central sawtooth waves

Frontal-central sawtooth waves resembled the typical sawtooth waves of REM sleep originally described in the 1960s (Jouvet et al., 1960; Schwartz and Fischgold, 1960; Berger et al., 1962). There is no universal agreement on defining criteria for sawtooth waves, but they are often described as medium-amplitude waves (≥ 20 μV) between 2 and 5 Hz (Jouvet et al., 1960; Berger et al., 1962; Yasoshima et al., 1984; Pinto et al., 2002; Vega-Bermudez et al., 2005), with a triangular shape (initial slow increase followed by a steep decrease; Rechtschaffen and Kales, 1968; Tafti et al., 1991; Rodenbeck et al., 2006) and a maximal frontal-central amplitude (Yasoshima et al., 1984; Broughton and Hasan, 1995). The presence of a notch, usually on the positive-to-negative slope, is occasionally mentioned (Foulkes and Pope, 1973; Rodenbeck et al., 2006). Sawtooth waves tend to occur in bursts (Geisler et al., 1987; Sato et al., 1997), herald the beginning of REM sleep (Sato et al., 1997), and often, but not necessarily, accompany bursts of rapid EMs (Berger et al., 1962; Schwartz, 1962; Sato et al., 1997; Takaharaa et al., 2009). The characteristics of frontal-central waves described herein are consistent with these observations. In addition, we provide several novel findings. First, using source modeling, we demonstrate a maximal involvement in medial prefrontal areas (midcingulate cortex, SMA, and the medial M1). We also identified a secondary temporo-occipital source associated with the sawtooth wave notch. Second, we showed that sawtooth waves are accompanied by an (in-phase) increase in high-frequency activity, suggesting an "activating" effect (i.e., increased neuronal firing; Steriade et al., 1996). The mechanism underlying these waves is thus likely different from NREM slow waves, which are associated with neuronal silence (OFF-periods). Finally, we were able to document a direct correlation between sawtooth waves and rapid EMs (the more sawtooth waves, the more subsequent EMs).

The characteristics of sawtooth waves raise the possibility that they are related to ponto-geniculo-occipital (PGO) waves, which were originally described in cats and consist of phasic electric potentials recorded from the pons, the lateral geniculate body (LGB), and the occipital cortex (Jouvet and Michel, 1959; Mikiten, 1961; Brooks and Bizzi, 1963; Mouret et al., 1963). They have also been mapped in limbic areas (amygdala, cingulate cortex, and hippocampus). Similar to sawtooth waves, PGO waves last between 60 and 360 ms (Callaway et al., 1987), appear at the NREM–REM sleep transition several seconds before the first rapid EM (Sato et al., 1997), occur in bursts (but isolated spikes are also observed; Jeannerod and Kiyono, 1969), and are typically, but not always, associated with trains of EMs (Morrison and Pompeiano, 1966). Although PGO waves have been recorded in many species, including nonhuman primates, their existence in humans remains controversial. A relation between sawtooth and PGO waves has been suggested based on the similar temporal characteristics, including their association with rapid EMs (Ishiguro et al., 1979; Takaharaa et al., 2009), but the different cortical distributions (frontal-central vs occipital) have hampered further analogies. The temporo-occipital component that we identified here may actually represent the cortical manifestation of human PGO waves. The increases in gamma power associated with sawtooth waves fit well with this hypothesis. Indeed, PGO waves have been referred to as "cortical activation waves" (Calvet and Calvet, 1968) because they are associated with increased neuronal firing in several cortical regions. Consistent with our findings, gamma power increases have been reported during rapid EM in frontal and central regions in REM sleep (Abe et al., 2008; Vijayan et al., 2017) and during phasic compared with tonic REM sleep (Corsi-Cabrera et al., 2008). Among the few case studies documenting potential human PGO-wave equivalents using intracranial recordings (Salzarulo et al., 1975; Lim et al., 2007; Fernández-Mendoza et al., 2009), one described the presence of simultaneous sawtooth waves in the scalp EEG in addition to increases in gamma activity (15–35 Hz), supporting the analogy between sawtooth and PGO waves (Fernández-Mendoza et al., 2009).

The correlation between sawtooth waves and rapid EM raises the question of whether sawtooth waves are directly involved in rapid EM generation. However, several points argue against this possibility. First, although saccades during wakefulness and REM sleep share many common features, including analogous ERP waveforms, the same phase reset of theta activity in medial temporal regions, a comparable modulation of neuronal firing rates (Andrillon et al., 2015), and the activation of similar brain regions (Hong et al., 1995; Ioannides et al., 2004), sawtooth waves do not accompany rapid EM during wakefulness. Second, whereas sawtooth waves clearly encompass the frontal and supplementary eye field, they also extend beyond these regions to V1, the SMA, and limbic regions (midcingulate, inferior/middle temporal cortex). Activations of these areas (Maquet et al., 1996; Nofzinger et al., 1997; Braun et al., 1998; Ioannides et al., 2004; Abe et al., 2008) and the LGB (Peigneux et al., 2001; Wehrle et al., 2005; Miyauchi et al., 2009) have been shown to differentiate brain activity during REM sleep from EM during wakefulness (Peigneux et al., 2001; Miyauchi et al., 2009). Our results suggest that these differences may be mediated by sawtooth waves, which are concomitant to EMs. Finally, the frontal-central topography is almost identical to some NREM potentials that are not associated with EMs, including vertex waves (Yasoshima et al., 1984;

Siclari et al., 2014) and high-frequency activity increases following type I slow waves (Siclari et al., 2014, 2018; Bernardi et al., 2018). During wakefulness, vertex potentials can be induced by sudden and intense stimuli of various sensory modalities, including pain. These potentials have been suggested to be related to stimulus saliency; that is, the ability of a stimulus to stand out from its surroundings (Legrain et al., 2011). Rapid EMs following sawtooth waves may thus constitute a reaction to a salient, possibly dreamed event. Consistent with this, PGO spikes can be induced in cats using sounds during both quiet wakefulness and REM and NREM sleep and may accompany a "startle-like" reaction (Bowker and Morrison, 1976), suggesting common behavioral significance of these potentials across states.

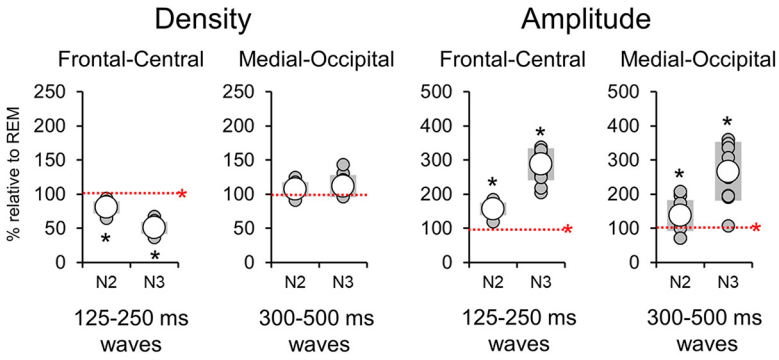

Figure 9. Relative variations in the density and amplitude of frontal-central and medial-occipital delta waves in N2 and N3 with respect to REM sleep. The dashed red line corresponds to the level observed in REM sleep (100%). Asterisk denotes significant effects at $p < 0.05$ (red for Friedman test for stage-effect, black for *post hoc* Wilcoxon signed rank tests).

Future studies should explore the relationship between sawtooth waves and midline frontal rhythms in the delta and theta frequency range that have been linked to cognitive processes during wakefulness and are phase coupled to gamma oscillations (Gevins et al., 1997; Sauseng et al., 2010; Fujisawa and Buzsáki, 2011). Also, given the prominent inferior temporal component of sawtooth waves, it would be of interest to evaluate how sawtooth waves relate to hippocampal delta rhythms of REM sleep that have been suggested to represent the human counterpart of hippocampal theta of mammalian REM sleep (Bódizs et al., 2001; Clemens et al., 2009; Moroni et al., 2012).

Medial-occipital slow waves

The second cluster of delta waves consisted of occipital slow waves (<2 Hz). This finding is consistent with previous work describing the maximal peak of low-delta activity in occipital areas during REM sleep (Tinguely et al., 2006; Ferrara and De Gennaro, 2011). Our results demonstrate that this source of delta activity is due to small, local slow waves that are not modulated by phasic REM and are associated with a suppression of gamma activity, similar to NREM slow waves (Siclari et al., 2014). We also show, for the first time, that occipital slow waves occur with a similar density, but different amplitudes, across all sleep stages. The amplitude of delta waves was higher in N3 relative to N2 or REM sleep and decreased across subsequent REM sleep periods. These variations may reflect neuromodulatory and sleep-dependent changes in synaptic density/strength that may affect the efficiency of neural synchronization during the generation and spreading of slow waves (Riedner et al., 2007; Tononi and Cirelli, 2014). Conversely, occipital slow wave density remained similar in NREM and REM sleep, but was higher than in wakefulness. Consistent with this, the occipital cortex, relative to other cortical areas, shows the smallest changes in SWA at NREM–REM sleep transitions (De Gennaro et al., 2002; Ferrara and De Gennaro, 2011). The relatively low frequency of occipital REM slow waves (<2 Hz) is consistent with the recent observation of a lower frequency of occipital NREM slow waves (~1 Hz) relative to anterior areas (Bersagliere et al., 2018).

Our observation of local occipital slow waves occurring at a similar rate across NREM and REM sleep is consistent with the hypothesis that slow waves in primary cortices play a role in sensory disconnection during sleep (Funk et al., 2016). However, with respect to slow waves recently described in mice (Funk et al., 2016), several differences should be noted. First, we did not observe SWA peaks in primary cortices other than V1. It is possible that local slow waves in other primary cortices may have been masked by the preponderant sawtooth activity in these areas. Indeed, in a recent study comparing SWA between REM and wakefulness, SWA activity was found to be higher in primary sensory cortices in REM sleep after excluding sawtooth waves (Baird et al., 2018). This possibility is also in part supported by the observation of a relative decrease in the frontal-central wave density in the 1–2 Hz range during REM periods dominated by "activating" sawtooth waves (i.e., phasic REM). Consistent with this view, recent work in animal models also described in REM sleep a 4 Hz prefrontal oscillation that was modulated separately from

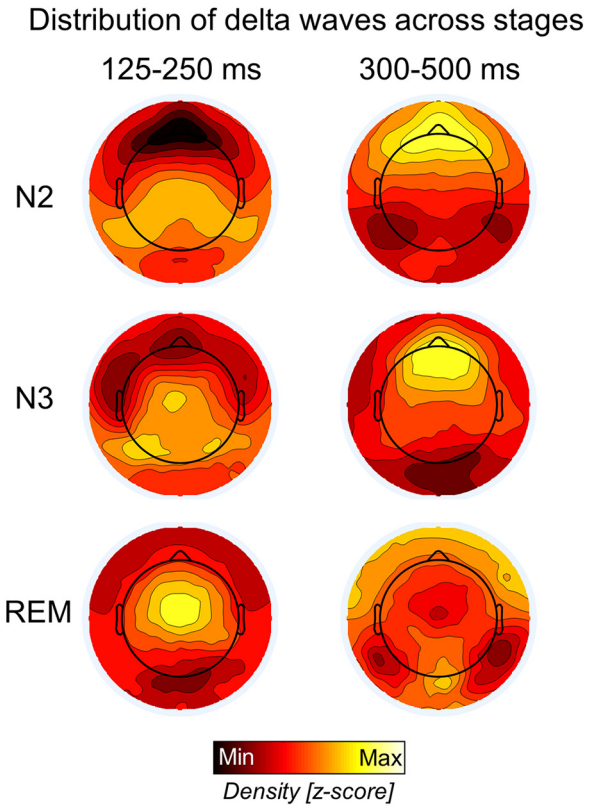

Figure 10. Relative topographic distribution of EEG waves with durations of 125–250 ms (left) and 300–500 ms (right) in N2, N3, and REM sleep. Density values were *z*-scored to facilitate comparison across stages. The strong frontal slow-wave activity in NREM sleep likely masks the smaller delta waves in posterior regions.

a <2 HZ oscillation after chronic sleep restriction (Kim et al., 2017). Second, in our study, we found that occipital slow waves, as opposed to sawtooth waves, were not modulated by phasic REM periods as in the animal study. This may be due to the different definitions of phasic REM periods that were used based on rapid EMs in humans and on whisking events (vibrissal EMG) in mice. However, we cannot exclude that slow waves observed in these two studies may represent distinct phenomena.

In several key aspects, these findings parallel the recent observation of two distinct slow-wave populations of in NREM sleep: widespread frontal-central type I slow waves, which are temporally related to high-frequency increases (micro-arousals), and diffusely distributed, local type II slow waves, which do not seem to be related to arousal systems (Siclari et al., 2014, 2018; Bernardi et al., 2018; Spiess et al., 2018). Therefore, both REM and NREM sleep appear to be characterized by frontal-central, potentially activating delta waves that stand out from the background of remaining of slow waves.

Limitations

We focused on a minority of delta waves that were typical of clusters emerging from topographical analyses. Therefore, there is a large "unclassified" background of delta waves that remains unexplored in the present study. Due to volume conduction affecting scalp EEG recordings, masking effects of prominent sawtooth waves with respect to other slow waves could not be avoided. Future human studies using intracranial recordings should explore the regional distribution of slow waves in REM sleep (primary vs secondary sensory cortices) and their association with off-periods.

Conclusions

Delta waves (≤4 Hz) are an integral feature of REM sleep. There appear to be at least two distinctive clusters of delta waves with different properties: a frontal-central cluster characterized by faster, activating sawtooth waves that share many characteristics with PGO waves described in animals and a medial-occipital cluster containing slow waves that are more similar to NREM sleep slow waves.

References

Abe T, Ogawa K, Nittono H, Hori T (2008) Neural generators of brain potentials before rapid eye movements during human REM sleep: a study using sLORETA. Clin Neurophysiol 119:2044–2053.

Andrillon T, Nir Y, Cirelli C, Tononi G, Fried I (2015) Single-neuron activity and eye movements during human REM sleep and awake vision. Nat Commun 6:7884.

Aserinsky E, Kleitman N (1953) Regularly occurring periods of eye motility, and concomitant phenomena, during sleep. Science 118:273–274.

Baird B, Castelnovo A, Riedner BA, Lutz A, Ferrarelli F, Boly M, Davidson RJ, Tononi G (2018) Human rapid eye movement sleep shows local increases in low-frequency oscillations and global decreases in high-frequency oscillations compared to resting wakefulness. eNeuro 5:ENEURO.0293–18.2018.

Berger RJ, Olley P, Oswald I (1962) The EEG, eye-movements and dreams of the blind. Q J Exp Psychol 14:183–186.

Bernardi G, Betta M, Cataldi J, Leo A, Haba-Rubio J, Heinzer R, Cirelli C, Tononi G, Pietrini P, Ricciardi E, Siclari F (2019) Visual imagery and visual perception induce similar changes in occipital slow waves of sleep. bioRxiv 1:532317.

Bernardi G, Siclari F, Yu X, Zennig C, Bellesi M, Ricciardi E, Cirelli C, Ghilardi MF, Pietrini P, Tononi G (2015) Neural and behavioral correlates of extended training during sleep deprivation in humans: evidence for local, task-specific effects. J Neurosci 35:4487–4500.

Bernardi G, Siclari F, Handjaras G, Riedner BA, Tononi G (2018) Local and widespread slow waves in stable NREM sleep: evidence for distinct regulation mechanisms. Front Hum Neurosci 12:248.

Bersagliere A, Pascual-Marqui RD, Tarokh L, Achermann P (2018) Mapping slow waves by EEG topography and source localization: effects of sleep deprivation. Brain Topogr 31:257–269.

Betta M, Gemignani A, Landi A, Laurino M, Piaggi P, Menicucci D (2013) Detection and removal of ocular artifacts from EEG signals for an automated REM sleep analysis. In: 2013 35th Annual International Conference of the IEEE Engineering in Medicine and Biology Society (EMBC), pp 5079–5082.

Betta M, Laurino M, Gemignani A, Landi A, Menicucci D (2015) A Classification method for eye movements direction during REM sleep trained on wake electro-oculographic recordings. In: 2015 37th Annual International Conference of the IEEE Engineering in Medicine and Biology Society (EMBC), pp 370–373.

Bódizs R, Kántor S, Szabó G, Szûcs A, Erõss L, Halász P (2001) Rhythmic hippocampal slow oscillation characterizes REM sleep in humans. Hippocampus 11:747–753.

Bowker RM, Morrison AR (1976) The startle reflex and PGO spikes. Brain Res 102:185–190.

Braun AR, Balkin TJ, Wesensten NJ, Gwadry F, Carson RE, Varga M, Baldwin P, Belenky G, Herscovitch P (1998) Dissociated pattern of activity in visual cortices and their projections during human rapid eye movement sleep. Science 279:91–95.

Brooks DC, Bizzi E (1963) Brain stem electrical activity during sleep. Arch Ital Biol 101:648–665.

Broughton R, Hasan J (1995) Quantitative topographic electroencephalographic mapping during drowsiness and sleep onset. J Clin Neurophysiol 12:372–386.

Callaway CW, Lydic R, Baghdoyan HA, Hobson JA (1987) Pontogeniculooccipital waves: spontaneous visual system activity during rapid eye movement sleep. Cell Mol Neurobiol 7:105–149.

Calvet J, Calvet MC (1968) Étude quantitative et organisation en fonction de la vigilance de l'activitéunitaire des diverses régions du cortex cérébral. Brain Res 10:183–199.

Clemens Z, Weiss B, Szucs A, Eross L, Rásonyi G, Halász P (2009) Phase coupling between rhythmic slow activity and gamma characterizes mesiotemporal rapid-eye-movement sleep in humans. Neuroscience 163:388–396.

Corsi-Cabrera M, Guevara MA, del Río-Portilla Y (2008) Brain activity and temporal coupling related to eye movements during REM sleep: EEG and MEG results. Brain Res 1235:82–91.

De Gennaro L, Ferrara M, Curcio G, Cristiani R, Bertini M (2002) Cortical EEG topography of REM onset: the posterior dominance of middle and high frequencies. Clin Neurophysiol 113:561–570.

Delorme A, Makeig S (2004) EEGLAB: an open source toolbox for analysis of single-trial EEG dynamics including independent component analysis. J Neurosci Methods 134:9–21.

Dement W, Kleitman N (1957) Cyclic variations in EEG during sleep and their relation to eye movements, body motility, and dreaming. Electroencephalogr Clin Neurophysiol 9:673–690.

Fattinger S, Kurth S, Ringli M, Jenni OG, Huber R (2017) Theta waves in children's waking electroencephalogram resemble local aspects of sleep during wakefulness. Sci Rep 7:11187.

Fernández-Mendoza J, Lozano B, Seijo F, Santamarta-Liébana E, Ramos-Platón MJ, Vela-Bueno A, Fernández-González F (2009) Evidence of subthalamic PGO-like waves during REM sleep in humans: a deep brain polysomnographic study. Sleep 32:1117–1126.

Ferrara M, De Gennaro L (2011) Going local: insights from EEG and stereo-EEG studies of the human sleep-wake cycle. Curr Top Med Chem 11:2423–2437.

Foulkes D, Pope R (1973) Primary visual experience and secondary cognitive elaboration in stage REM: a modest confirmation and an extension. Percept Mot Skills 37:107–118.

Fujisawa S, Buzsáki G (2011) A 4 hz oscillation adaptively synchronizes prefrontal, VTA, and hippocampal activities. Neuron 72:153–165.

Funk CM, Honjoh S, Rodriguez AV, Cirelli C, Tononi G (2016) Local slow waves in superficial layers of primary cortical areas during REM sleep. Curr Biol 26:396–403.

Geisler P, Meier-Ewert K, Matsubayshi K (1987) Rapid eye movements, muscle twitches and sawtooth waves in the sleep of narcoleptic patients and controls. Electroencephalogr Clin Neurophysiol 67:499–507.

Gevins A, Smith ME, McEvoy L, Yu D (1997) High-resolution EEG mapping of cortical activation related to working memory: effects of task difficulty, type of processing, and practice. Cereb Cortex 7:374–385.

Hong CC, Gillin JC, Dow BM, Wu J, Buchsbaum MS (1995) Localized and lateralized cerebral glucose metabolism associated with eye movements during REM sleep and wakefulness: a positron emission tomography (PET) study. Sleep 18:570–580.

Huber R, Ghilardi MF, Massimini M, Tononi G (2004) Local sleep and learning. Nature 430:78–81.

Huber R, Ghilardi MF, Massimini M, Ferrarelli F, Riedner BA, Peterson MJ, Tononi G (2006) Arm immobilization causes cortical plastic changes and locally decreases sleep slow wave activity. Nat Neurosci 9:1169–1176.

Hung CS, Sarasso S, Ferrarelli F, Riedner B, Ghilardi MF, Cirelli C, Tononi G (2013) Local experience-dependent changes in the wake EEG after prolonged wakefulness. Sleep 36:59–72.

Iber C, Ancoli-Israel S, Chesson AL, Quan SF (2007) The AASM manual for the scoring of sleep and associated events: Rules, terminology and technical specifications. Darien, IL: American Academy of Sleep Medicine.

Ioannides AA, Corsi-Cabrera M, Fenwick PBC, del Rio Portilla Y, Laskaris NA, Khurshudyan A, Theofilou D, Shibata T, Uchida S, Nakabayashi T, Kostopoulos GK (2004) MEG tomography of human cortex and brainstem activity in waking and REM sleep saccades. Cereb Cortex 14:56–72.

Ishiguro T, Hanamura S, Otaka T (1979) The saw-tooth wave associated with small nystagmus: a study on a narcoleptic patient and her family. Sleep Res 8:195.

Jeannerod M, Kiyono S (1969) Unitary discharge of pontine reticular formation and phasic ponto-geniculo-occipital activity in the cat under reserpine. Brain Res 12:112–128.

Johns MW (1991) A new method for measuring daytime sleepiness: the epworth sleepiness scale. Sleep 14:540–545.

Jouvet M, Michel F (1959) Corrélations électromyographiques du sommeil chez le chat décortiqué et mésencéphalique chronique. Comptes Rendus la Societe′ Biol 153:422–425.

Jouvet M, Michel F, Mounier D (1960) Analyse électroencéphlographique comparée du sommeil physiologique chez le chat et chez l'homme. Rev Neurol (Paris) 103:189–205.

Kim B, Kocsis B, Hwang E, Kim Y, Strecker RE, McCarley RW, Choi JH (2017) Differential modulation of global and local neural oscillations in REM sleep by homeostatic sleep regulation. Proc Natl Acad Sci U S A 114:E1727–E1736.

Legrain V, Iannetti GD, Plaghki L, Mouraux A (2011) The pain matrix reloaded: a salience detection system for the body. Prog Neurobiol 93:111–124.

Lim AS, Lozano AM, Moro E, Hamani C, Hutchison WD, Dostrovsky JO, Lang AE, Wennberg RA, Murray BJ (2007) Characterization of REM sleep associated ponto-geniculo-occipital waves in the human pons. Sleep 30:823–827.

Maquet P, Péters J, Aerts J, Delfiore G, Degueldre C, Luxen A, Franck G (1996) Functional neuroanatomy of human rapid-eye-movement sleep and dreaming. Nature 383:163–166.

Massimini M, Huber R, Ferrarelli F, Hill S, Tononi G (2004) The sleep slow oscillation as a traveling wave. J Neurosci 24:6862–6870.

Mensen A, Riedner B, Tononi G (2016) Optimizing detection and analysis of slow waves in sleep EEG. J Neurosci Methods 274:1–12.

Mikiten T, Niebyl P, Hendley C (1961) EEG desynchronization during behavioural sleep associated with spike discharge from the thalamus of the cat. Federation proceedings 20:327.

Miyauchi S, Misaki M, Kan S, Fukunaga T, Koike T (2009) Human brain activity time-locked to rapid eye movements during REM sleep. Exp Brain Res 192:657–667.

Moroni F, Nobili L, De Carli F, Massimini M, Francione S, Marzano C, Proserpio P, Cipolli C, De Gennaro L, Ferrara M (2012) Slow EEG rhythms and inter-hemispheric synchronization across sleep and wakefulness in the human hippocampus. Neuroimage 60:497–504.

Morrison AR, Pompeiano O (1966) Vestibular influences during sleep. IV. Functional relations between vestibular nuclei and lateral geniculate nucleus during desynchronized sleep. Arch Ital Biol 104:425–458.

Mouret J, Jeannerod M, Jouvet M (1963) L'activite electrique du systeme visuel au cours de la phase paradoxale du sommeil chez le chat. J Physiol 55:305–306.

Nichols TE, Holmes AP (2002) Nonparametric permutation tests for functional neuroimaging: a primer with examples. Hum Brain Mapp 15:1–25.

Nir Y, Staba RJ, Andrillon T, Vyazovskiy VV, Cirelli C, Fried I, Tononi G (2011) Regional slow waves and spindles in human sleep. Neuron 70:153–169.

Nofzinger EA, Mintun MA, Wiseman M, Kupfer DJ, Moore RY (1997) Forebrain activation in REM sleep: an FDG PET study. Brain Res 770:192–201.

Pearl PL, LaFleur BJ, Reigle SC, Rich AS, Freeman AA, McCutchen C, Sato S (2002) Sawtooth wave density analysis during REM sleep in normal volunteers. Sleep Med 3:255–258.

Peigneux P, Laureys S, Fuchs S, Delbeuck X, Degueldre C, Aerts J, Delfiore G, Luxen A, Maquet P (2001) Generation of rapid eye movements during paradoxical sleep in humans. Neuroimage 14:701–708.

Pinto LR Jr, Peres CA, Russo RH, Remesar-Lopez AJ, Tufik S (2002) Sawtooth waves during REM sleep after administration of haloperidol combined with total sleep deprivation in healthy young subjects. Braz J Med Biol Res 35:599–604.

Rechtschaffen A, Kales A (1968) A manual of standardized terminology, techniques and scoring system for sleep stages of human subjects. Bethesda, MD: National Institutes of Health publication.

Riedner BA, Vyazovskiy VV, Huber R, Massimini M, Esser S, Murphy M, Tononi G (2007) Sleep homeostasis and cortical synchronization: III. A high-density EEG study of sleep slow waves in humans. Sleep 30:1643–1657.

Rodenbeck A, Binder R, Geisler P, Danker-Hopfe H, Lund R, Raschke F, Weeβ H, Schulz H (2006) A review of sleep EEG patterns. Part I: a compilation of amended rules for their visual recognition according to rechtschaffen and kales. Somnologie 10:159–175.

Salzarulo P, Pelloni G, Lairy GC (1975) Semeiologie electrophysiologique du sommeil de jour chez l'enfant de 7 a 9 ans. Electroencephalogr Clin Neurophysiol 38:473–494.

Sato S, McCutchen C, Graham B, Freeman A, von Albertini-Carletti I, Alling DW (1997) Relationship between muscle tone changes, sawtooth waves and rapid eye movements during sleep. Electroencephalogr Clin Neurophysiol 103:627–632.

Sauseng P, Griesmayr B, Freunberger R, Klimesch W (2010) Control mechanisms in working memory: a possible function of EEG theta oscillations. Neurosci Biobehav Rev 34:1015–1022.

Schwartz BA (1962) EEG et mouvements oculaires dans le sommeil de nuit. Electroencephalogr Clin Neurophysiol 14:126–128.

Schwartz BA, Fischgold H (1960) Introduction à l'étude polygraphique du sommeil de nuit (mouvements oculaires et cycles de sommeil). Vie Medicale au Canada Français 41:39–46.

Siclari F, Tononi G (2017) Local aspects of sleep and wakefulness. Curr Opin Neurobiol 44:222–227.

Siclari F, Bernardi G, Riedner BA, LaRocque JJ, Benca RM, Tononi G (2014) Two distinct synchronization processes in the transition to sleep: a high-density electroencephalographic study. Sleep 37:1621–1637.

Siclari F, Baird B, Perogamvros L, Bernardi G, LaRocque JJ, Riedner B, Boly M, Postle BR, Tononi G (2017) The neural correlates of dreaming. Nat Neurosci 20:872–878.

Siclari F, Bernardi G, Cataldi J, Tononi G (2018) Dreaming in NREM sleep: a high-density EEG study of slow waves and spindles. J Neurosci 38:9175–9185.

Snyder EW, Dustman RE, Johnson RL (1978) Sawtooth waves: concomitants of rapid eye movement sleep in monkeys. Electroencephalogr Clin Neurophysiol 45:111–113.

Spiess M, Bernardi G, Kurth S, Ringli M, Wehrle FM, Jenni OG, Huber R, Siclari F (2018) How do children fall asleep? A high-density EEG study of slow waves in the transition from wake to sleep. Neuroimage 178:23–35.

Steriade M, Nuñez A, Amzica F (1993) A novel slow ($<$1 Hz) oscillation of neocortical neurons in vivo: depolarizing and hyperpolarizing components. J Neurosci 13:3252–3265.

Steriade M, Amzica F, Contreras D (1996) Synchronization of fast (30–40 Hz) spontaneous cortical rhythms during brain activation. J Neurosci 16:392–417.

Steriade M, Timofeev I, Grenier F (2001) Natural waking and sleep states: a view from inside neocortical neurons. J Neurophysiol 85:1969–1985.

Tafti M, Olivet H, Billiard M (1991) Phasic events in narcolepsy and sleep

apnea syndrome. In: Phasic Events and Dynamic Organization of Sleep, pp 151–166. New York: Raven Press.

Takaharaa M, Kanayamab S, Horib T (2009) Co-occurrence of sawtooth waves and rapid eye movements during REM sleep. Int J Bioelectromagn 11:144–148.

Tinguely G, Finelli LA, Landolt HP, Borbély AA, Achermann P (2006) Functional EEG topography in sleep and waking: state-dependent and state-independent features. Neuroimage 32:283–292.

Tononi G, Cirelli C (2014) Sleep and the price of plasticity: from synaptic and cellular homeostasis to memory consolidation and integration. Neuron 81:12–34.

Valderrama M, Crépon B, Botella-Soler V, Martinerie J, Hasboun D, Alvarado-Rojas C, Baulac M, Adam C, Navarro V, Le Van Quyen M (2012) Human gamma oscillations during slow wave sleep. PLoS One 7:e33477.

Vega-Bermudez F, Szczepanski S, Malow B, Sato S (2005) Sawtooth wave density analysis during REM sleep in temporal lobe epilepsy patients. Sleep Med 6:367–370.

Vijayan S, Lepage KQ, Kopell NJ, Cash SS (2017) Frontal beta-theta network during REM sleep. Elife 6:e18894.

Vyazovskiy VV, Olcese U, Hanlon EC, Nir Y, Cirelli C, Tononi G (2011) Local sleep in awake rats. Nature 472:443–447.

Vyazovskiy VV, Cui N, Rodriguez AV, Funk C, Cirelli C, Tononi G (2014) The dynamics of cortical neuronal activity in the first minutes after spontaneous awakening in rats and mice. Sleep 37:1337–1347.

Wehrle R, Czisch M, Kaufmann C, Wetter TC, Holsboer F, Auer DP, Pollmächer T (2005) Rapid eye movement-related brain activation in human sleep: a functional magnetic resonance imaging study. Neuroreport 16:853–857.

Yasoshima A, Hayashi H, Iijima S, Sugita Y, Teshima Y, Shimizu T, Hishikawa Y (1984) Potential distribution of vertex sharp wave and saw-toothed wave on the scalp. Electroencephalogr Clin Neurophysiol 58:73–76.